Miniaturized quantum systems for inertial measurement units

A. Kassner[1], L. Diekmann[1], C. Künzler[1], J. Petring[1], N. Droese[1], F. Dencker[1], H. Heine[2], S. Abend[2], M. Gersemann[2], E. M. Rasel[2], W. Herr[3], C. Schubert[3] and M. C. Wurz[1]

[1] Institute of Micro Production Technology (IMPT), Leibniz University Hannover
An der Universität 2
30823 Garbsen
GERMANY

[2] Institute of Quantum Optics (IQO), Leibniz University Hannover
Welfengarten 1
30167 Hannover
GERMANY

[3] German Aerospace Center (DLR), Institute for Satellite Geodesy and Inertial Sensing
Callinstr. 30b
30167 Hannover
GERMANY

2023 DGON Inertial Sensors and Systems (ISS) | 979-8-3503-4724-1/23/$31.00 ©2023 IEEE | DOI: 10.1109/ISS58390.2023.10361909

Inertial Sensors and Systems 2023
Braunschweig, Germany

Abstract

We present the development of an atom chip system along with associated peripherals for a six-axis quantum inertial navigation sensor based on atom interferometry. Based on quantum mechanical measurement concepts, these sensors are expected to have high sensitivity and superior long-term stability compared to conventional inertial sensors. Furthermore, they enable offset-free absolute measurement. However, the low measurement rate proves to be a disadvantage. Compared to classical inertial sensors, quantum inertial navigation sensors thus exhibit complementary features, so that a combination of these two methods appears promising. The use of inertial measurement systems on board of aircraft or satellites is usually accompanied by limitations in size, payload and power consumption. To meet these requirements, we address both the atom chip system itself and the necessary environment in the form of pumps and vacuum enclosures which are crucial parts of the sensor head.

1. Introduction

Inertial measurement units (IMU), which determine the motion of an object in all three spatial directions by integrating the measured accelerations and rotation rates, enable autonomous navigation without an external reference signal. However, measurement noise and sensor errors, which lead to position errors that increase over time, prove to be a challenge. The support of the IMU by means of GPS (GNSS) requires a corresponding availability, which is not given in every situation.

This is where our research activities come in. A consortium consisting of the Institute of Microproduction Technology (IMPT), the Institute of Quantum Optics (IQO), the Institute of Geodesy (IFE) and partners from industry is developing quantum inertial sensors based on atom chips, which are intended to support conventional IMU.

Compared to conventional inertial sensors, quantum inertial sensors are expected to have high sensitivity and better long-term stability. Another advantage is the offset-free absolute measurement. The measurement rate, on the other hand, is lower. Quantum inertial navigation sensors therefore exhibit a complementary feature compared to classical inertial sensors. For the reasons mentioned above, a combination of these two sensor types seems to be very reasonable.

The IMPT is focusing on the development of the atom chip system and the associated peripherals to be used in the six-axis quantum inertial navigation sensor. The atom chip, in

combination with laser cooling and other external coils, forms a magneto-optical trap for trapping and manipulating neutral atoms. The atom chip itself contains microtechnologically manufactured conductive tracks through which a current flows and magnetic fields are induced. Such atom chip systems are already used in single-axis atom interferometers with the scope of measuring $\vec{g}$ by absolute gravimetry [1], [2]. The principle of operation is shown in figure 1.

The wave properties of atoms are used to investigate the frictionless free fall of atoms. Position determination is performed using a CCD camera, which detects the spatial absorption of a light pulse to obtain information about the number of atoms, but the accuracy is limited by wavefront effects [1], [2], [3], [4]. The use of Bose-Einstein condensates (BEC) is intended to provide improved drift and accuracy performance by reducing wavefront effects.

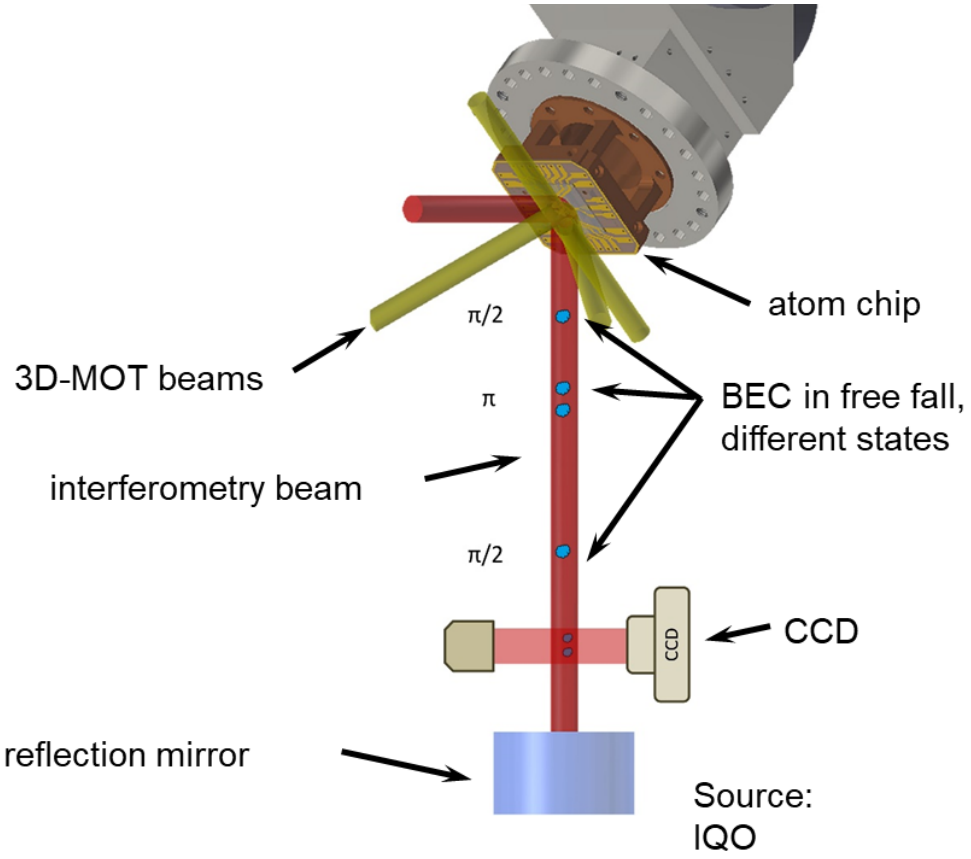

Figure 1. Detail from QG-1 matter wave interferometer [2].

The working principle of the atom interferometer is the quantum mechanical analogue of the Mach-Zehnder interferometer. To implement beam splitters and mirrors, light pulses manipulate atomic states [6], [7]. The space-time diagram of a Mach-Zehnder-type atom

interferometer under the influence of the gravitational acceleration $\vec{g}$ is shown in figure 2. The temporally displaced red wavy lines are the light pulses where the π/2 pulse splits the atomic wave function while the π-pulse serves to mirror the imprinted momentum and reunite the trajectories [8].

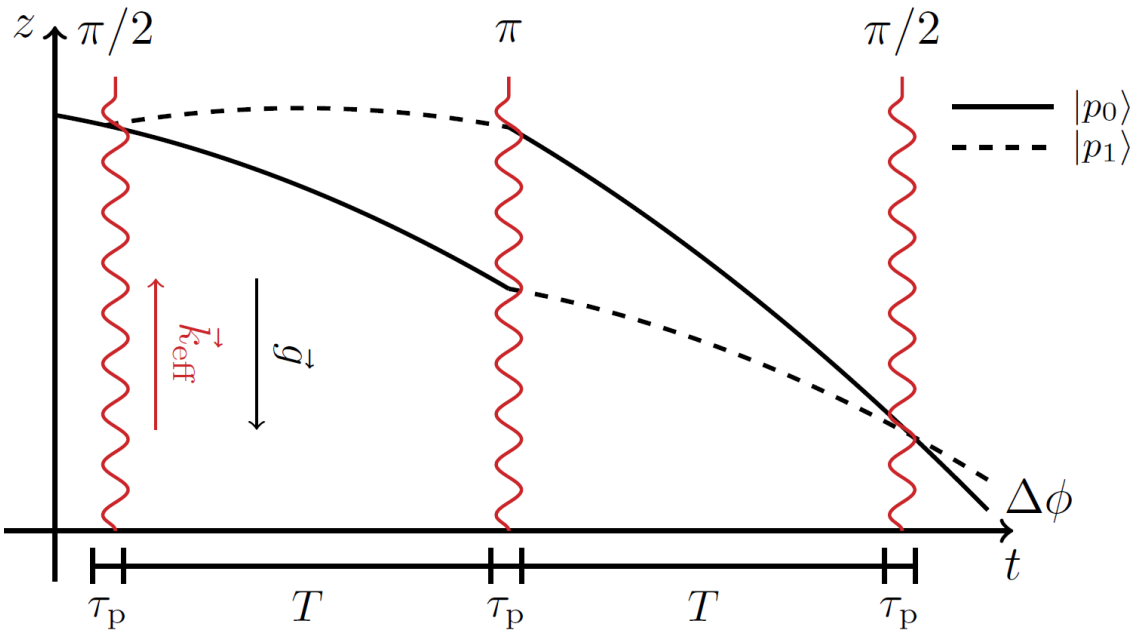

Figure 2. Space-time diagram of a Mach-Zehnder-type atom interferometer under the influence of the gravitational acceleration $\vec{g}$.(courtesy of Matthias Gersemann [8])

The advantage over laser gravimeters lies in the fact that the atom gravimeter does not require complex mechanics like a freely falling corner-cube mirror [5]; in addition, it works without external calibration.

For use as an inertial measurement unit, the project consortium is aiming for a setup implementing a multi-axis concept [9]. Instead of relying on multiple BEC sources, the system uses a single BEC source to generate two simultaneous interferometers for differentiation between rotation and acceleration. For this purpose, the system relies on an atom chip and three light fields arranged perpendicular to each other. Three sequential measurements are necessary to determine all three acceleration and rotation components, each with an initial splitting along one of the three axes [9].

The current design approach of the sensor head of an IMU based on the multi-axis concept in which the atom chip will be used is shown in figure 3.

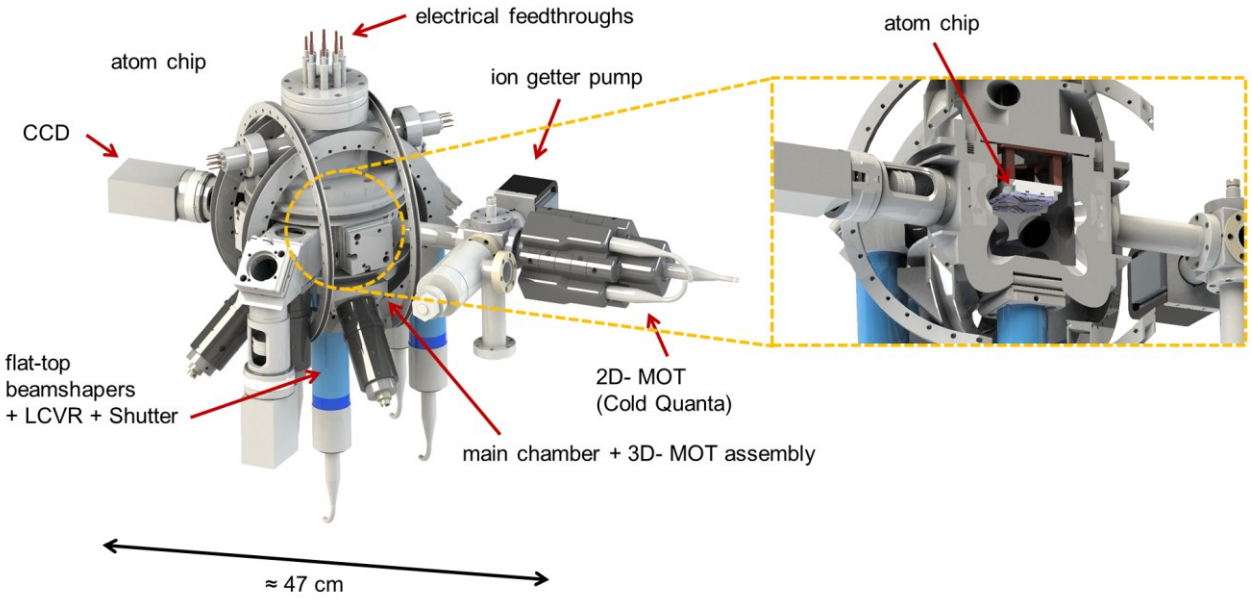

Figure 3. Design of the sensor head for an IMU based on the multi-axis concept and detailed view with atom chip system.

The miniaturization of atom chips as a source of BEC in transportable quantum gravimeters presents a manufacturing challenge with respect to chip integration. The atom chip is operated under ultra-high vacuum conditions, so low outgassing materials and non-adhesive interconnect techniques are used. Furthermore, optical access to the chip surface for laser interferometry and laser cooling is necessary to realize a magneto-optical trap. The fabrication of the atom chip is based on micro technology while non-adhesive techniques such as transient liquid phase diffusion bonding are used to connect the chip to a carrier system. While the atom chip is already available as a miniaturized component, the remaining parts of the overall system are still comparatively large components.

In addition to the atom chip, miniaturization of the vacuum system towards a UHV micro chamber is also performed. In a first step, the compactification is done by using 3D metal printing in combination with standardized CF connectors. This will enable compatibility with CF-based (macroscopic) vacuum systems. In addition to the vacuum housing, the vacuum periphery is also addressed during miniaturization. As a perspective, we anticipate a realization on chip level. In analogy to the established micro-electro-mechanical systems (MEMS), we strive for a miniaturized quantum system (MQS). The individual subsystems required for this are currently under development at the IMPT. Figure 4 shows a preview of a potential miniaturized quantum system.

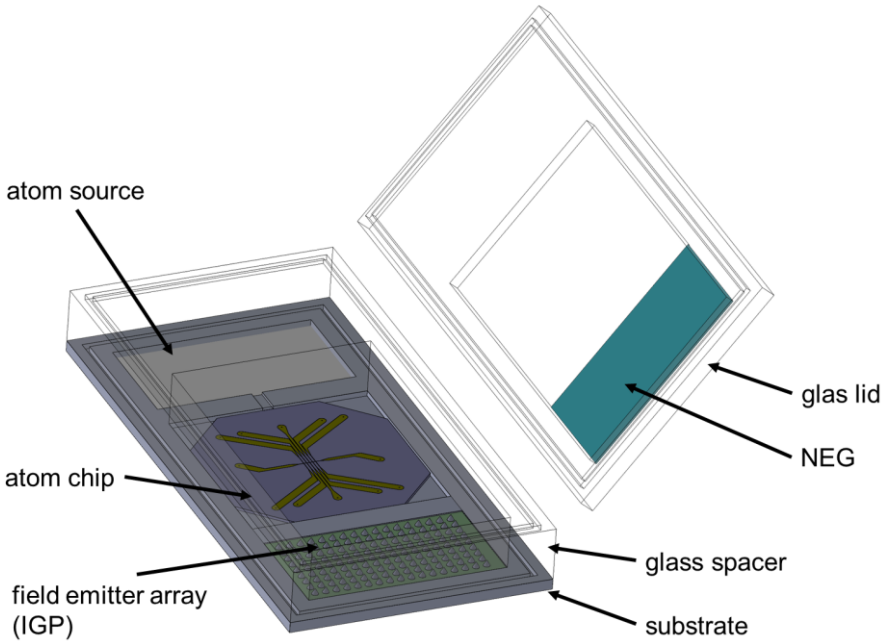

Figure 4: Preview of a potential miniaturized quantum system.

We consider the MQS as an integration platform, which combines all necessary functions for the operation of a quantum system. In addition to the core component (e.g. atom chip), all peripheral systems are also included.

2. Atom chip System

The operating principle of the atom chip will be presented in the following on the basis of the first generation of atom chips developed at the IMPT. The system shown in figure 5a) consists of three levels of conductors. To visualize the individual conductor tracks, the atom chip is shown transparently in figure 5b) and the conductors are color-coded. The atom chip has thin-film conductors, while the mesoscopic structures within the carrier system are in the form of wires. The individual conductor tracks or the combination of several conductor tracks are designated with letters due to their shape. Thus, the thin-film structure of the atom chip is referred to as the Z-structure while the mesoscopic conductors are treated as the U- and H-configuration. The respective active conductor tracks and the current flow direction determine the resulting magnetic field configuration. Figure 6 shows the different steps up to the generation of the BEC. In the first step of the magneto-optical trap, laser cooling and the magnetic field in the U-configuration are active. In this state, the current flows through the central H-conductor (marked yellow in figure 6) and the lateral H-conductors (marked red in figure 6) in opposite directions. The trapping and cooling of the atoms is based on the fact that the photons of the laser constantly "push" the atoms into the center of the trap,

defined by the magnetic field configuration. The MOT reaches temperatures of ~200 µK. Since this temperature is still too high for Bose-Einstein condensation, the optical molasses takes place in a second step. In this phase, only the lasers are on but no magnetic fields (not in the figure). This results in further cooling of the atoms, down to the level of 4 µK.

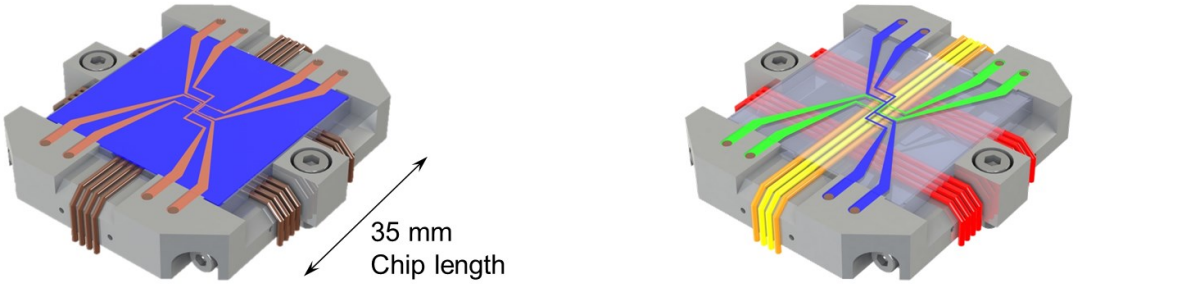

a) Model of the atom chip system

b) Visualization of the conductor track levels

Figure 5. Setup of the Atom Chip System [10].

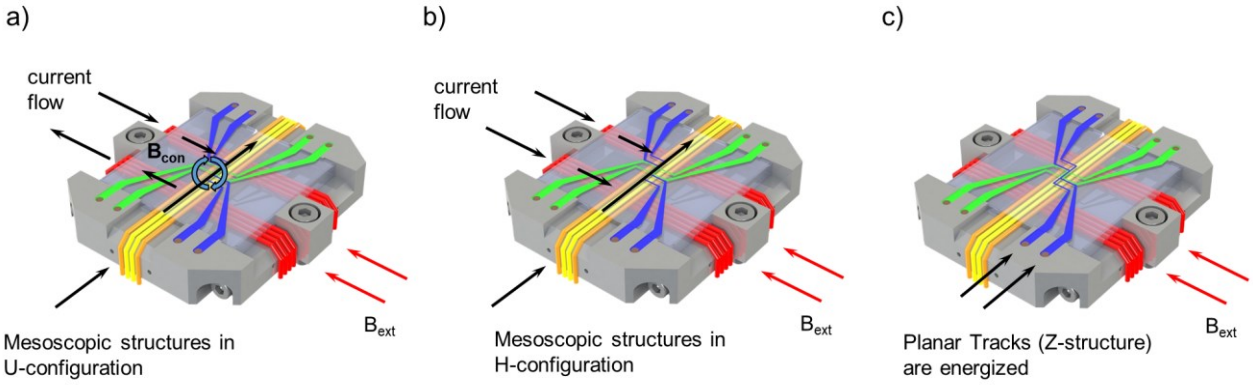

Figure 6. Setup of the atom chip System: Generation of BEC [10].

Subsequently, the atoms are trapped on the basis of the Zeeman effect by purely magnetic forces. For this purpose, the conductors are operated in an H-configuration as shown in figure 6b). For this, the current flows through the lateral H-conductors now point in the same direction. The result is the first large volume initial magnetic trap. The planar tracks of the atom chip in Z configuration are now put into operation (figure 6c)) and provide the transfer into the final magnetic trap. The trap is compressed and pulled closer to the chip. Evaporative cooling with the RF antennas in the atom chip (shown in green in figure 6) is used to selectively remove the highest energy atoms for cooling to T_c for Bose-Einstein condensation.

3.2. Atom chip structure and manufacturing

The atom chip as a core component is subject to boundary conditions during development and manufacture, the observance of which is indispensable for operation. The operating principle shown in figure 1 requires a reflective and thus flat surface of the atom chip for laser interferometry. Likewise, a free optical access for laser cooling is assumed. [11]

The state of the art in microsystem technology, which is also used in atom chip fabrication, consists of embedding the surface-applied conductor tracks with polyimide [12]. The surface is subsequently coated with a mirror coating [13]. An alternative process, which was developed in the context of atom chip production, involves the use of so-called transfer coatings. In this approach, the mirror coating is not applied directly to the atom chip surface but to a carrier substrate. The latter is then bonded to the atom chip by means of an epoxy, with the coated side facing the atom chip. The carrier substrate is then removed so that the mirror coating remains on the atom chip surface. [11], [14] Since the atom chip is used under ultra-high vacuum conditions, the large-area use of polymers and adhesives used in both processes can be disadvantageous, as outgassing effects can occur. With this in the mind, our approach relies on conductive traces embedded in the substrate. The layered structure of the atom chip is shown in figure 7.

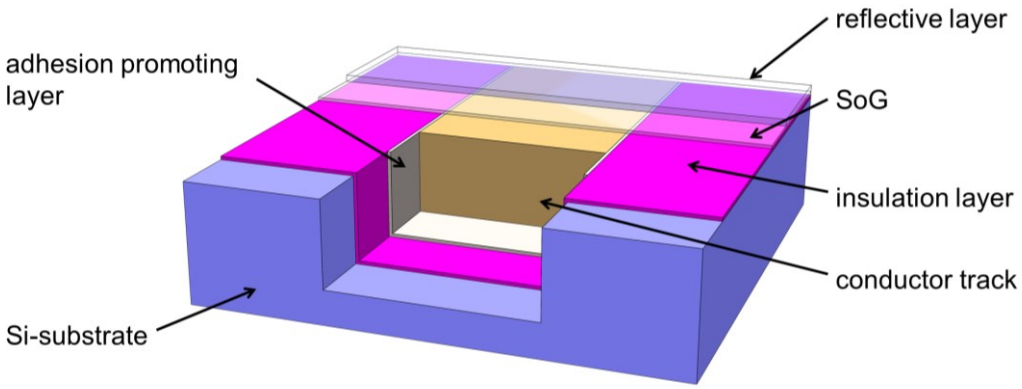

Figure 7. Layer structure of the atom chip.

The substrate is a silicon wafer into which a 10-20 µm deep trench has been etched, which is then filled with the conductor track material and finally planarized. An additional adhesion promoter layer such as titanium or chromium is used to improve the layer adhesion of the conductor track and to prevent delamination. The individual process steps are shown in figure 8 and explained below.

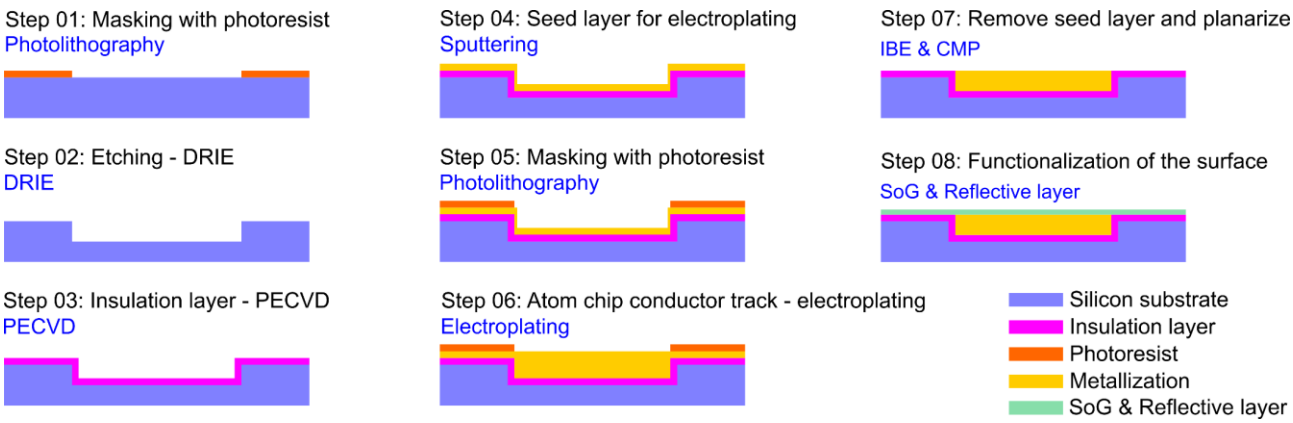

Figure 8. Process flow for the manufacture of the atom chip.

After cleaning, a photomask is applied to the silicon wafer by means of photolithography, in which a photoresist is spun on, exposed through a structured glass mask and developed. In this way, the image of the photomask is transferred 1:1 into the photoresist. In a second process step, the areas of the silicon wafer that are not covered by photoresist are subjected to an etching process. This is deep reactive ion etching, a nearly anisotropic etching process that can be used to create trenches for the conductor tracks as well as electrical feedthroughs through the entire thickness of the silicon wafer. Since silicon is a semiconducting material with a state-dependent electrical conductivity, an insulating layer is deposited in a third step using plasma-enhanced chemical vapor deposition (PECVD). In this way, SiO_2 and Si_3N_4 layer stacks are created. The conductor tracks of the atom chip completely fill the etched trench. Due to the layer thickness, electrodeposition is used for this purpose. However, the basic prerequisite for this is a conductive seed layer. By sputtering, a thin adhesion promoter layer is applied first, followed by the actual seed layer of gold or copper in a fourth step. To ensure that the growth only occurs in the trenches and not over the entire surface during electrodeposition, a photomask is applied again in the fifth step before the conductors are deposited in the sixth step. Due to elevations of the electric field in the area of the edges, an inhomogeneous growth occurs during the electrodeposition, which manifests itself in a strong overgrowth in the area of the conductor track edges. This phenomenon is illustrated in figure 9a). Therefore, in the seventh step, the seed layer is first removed by ion beam etching (IBE) before the surface is planarized by chemical mechanical polishing (CMP). Figure 9b) shows the cross-section of the conductor track after the CMP process. For this purpose, atom chip was cut, the sample was subsequently embedded in a casting compound, and the cross-section was analysed with a scanning electron microscope (SEM).

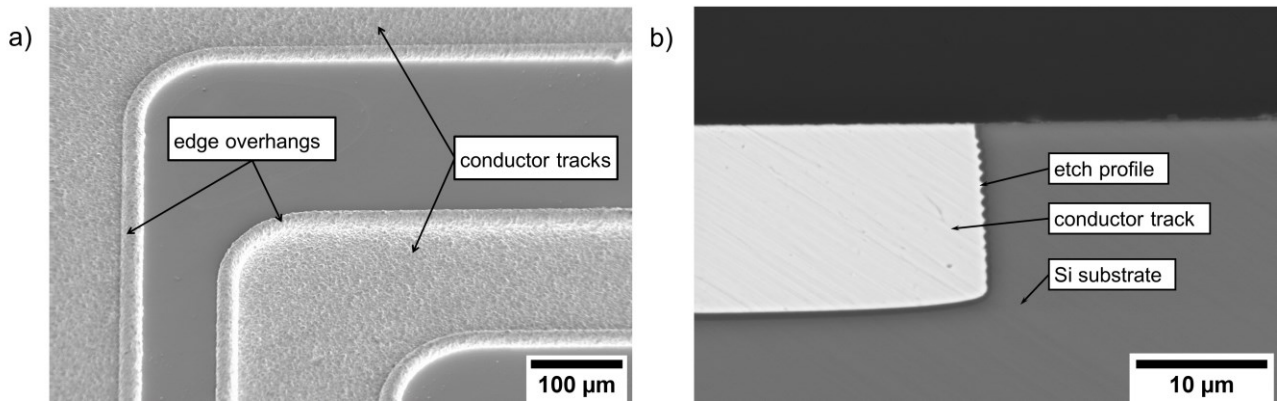

Figure 9. a) SEM image of the surface of the atom chip after electroplating.
b) SEM image of the cross section after planarization by CMP.

The criteria for the evaluation include the levelling of the conductor tracks as well as possible cavities within the conductor track or trenches between the substrate and the conductor track. A closer look also reveals the etching profile of the DRIE process and the approximately one-micrometer-thick insulation layer. Due to the alternating etch behavior of the DRIE process, the sidewall of the trench has a wavy profile. This can be challenging for conformal coating of the insulation layer, but at the same time it improves adhesion of the conductor track by providing interlocking. The eighth and final step initially involves the application of spin on glass (SoG). In the present case, this is 500 nm thick, levels local unevenness and provides the surface with an additional insulation layer. Finally, the reflective layer is applied, for example by ion beam sputtering (IBS).

3.2. Atom chip mounting and development to the multilayer system

The production of the atom chip takes place at wafer level. At the end of the process chain, the wafer is separated into chips by a separation grinding process. These chips now have to be joined onto a carrier system. Since the operation of the atom chip is influenced by external magnetic fields, only non-magnetic materials are used in the entire atom chip system. The use of conductive materials, apart from the actual conductor tracks, is also avoided in order to suppress eddy currents. The material used is therefore Shapal™, an AlN ceramic. This is characterized by good machinability, high thermal conductivity and good electrical insulation properties. The carrier not only has the task of holding the atom chip and providing space for the electrical feedthroughs, but it also contains the mesoscopic structures in the form of wires. These are fixed in guide trenches. Non-adhesive bonding techniques are used to join the atom chip to the carrier. For this purpose, we use transient liquid phase diffusion bonding (TLPD-bonding) with the material combination gold-indium. Figure 10 shows the layered structure of the joint and the completed system. This system

represents the first atom chip system manufactured at IMPT. Ceramabond^{TM} 835-M was used to bond the ceramic components; our current systems do not use adhesives at all.

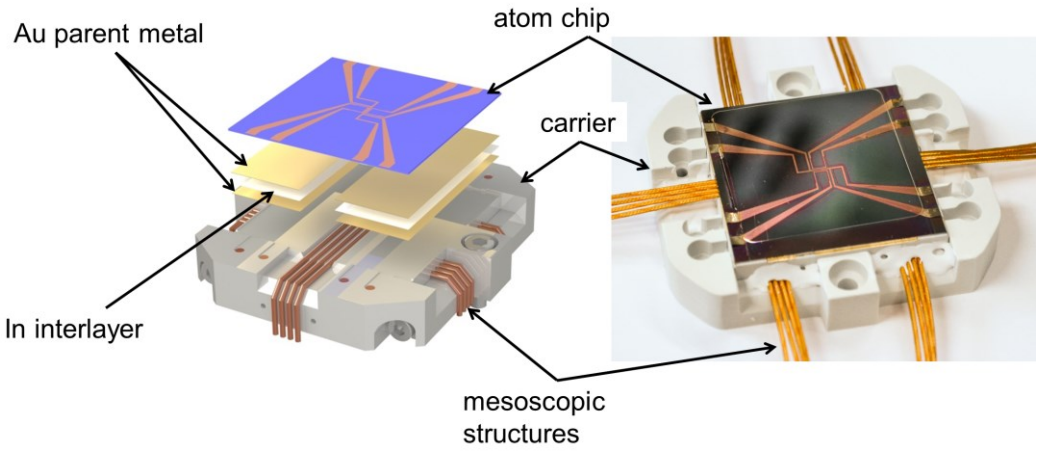

Figure 10. Layered structure of the joint and the completed system.

The components to be joined are first coated with the gold parent metal by means of sputtering. Shadow masks are used to structure the coating. The indium interlayer is introduced in foil form. The joining partners are brought into contact with each other and a temperature and pressure are applied. The melting temperature of the indium interlayer is 156°C. Melting and homogenization of the interlayer leads to a reaction with the parent metal and intermetallic compounds are formed, which have a higher melting point. When the interlayer is completely transformed, isothermal solidification occurs. Hence the name "transient liquid phase", because the Liquid solidifies before cooling down. This is a joining process with a comparatively low process temperature, which is important because the atom chip consists of different materials with different coefficients of thermal expansion, which can result in the risk of layer delamination if the temperature is excessive. The remelting temperature is over 500 °C depending on the alloy composition. Due to the thickness of the interlayer, the joint layer is comparatively tolerant to surface defects and offers good thermal conductivity to dissipate the joule heat of the atom chip.

The electrical contacting of the first atom chip generation is still made via surface contacts, so that optical access was blocked in certain spatial directions. The current generation is fully contacted from the backside to ensure full optical access, as shown in figure 10. For this purpose, we use pins made of copper with a 5-axis CNC machine. In the area of contacting, a two-stage etch is performed through the silicon substrate, which resembles a counterbore when viewed in cross-section. The etching with the larger diameter is

sufficiently dimensioned to accommodate the pin head. The etching with the smaller diameter is used to pass through the electrically conductive layer. It is also used for evacuation to prevent any virtual leakage in the vacuum.

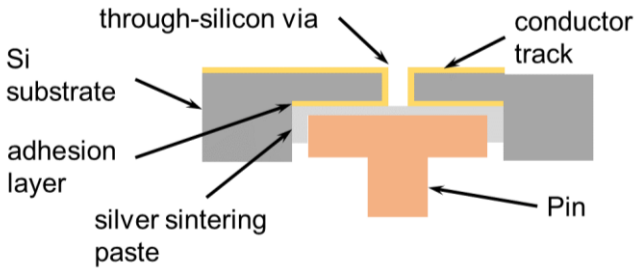

Figure 10. Schematic overview of the pin connection.

Silver sintering paste is used as a non-adhesive connection technique for the pins. This can be scraped into the feedthroughs before the pins are placed. The application of pressure is not mandatory, the temperature in the joining process is 235 °C. The result of the joining process is a silver framework after solvent outgassing. Adhesion takes place to silver or gold surfaces. This joining technique can also be used as an alternative to TLPD bonding for the atom chips themselves. The melting point is 961°C.

The integration density can be increased by multilayer systems, for example, our current setup uses two silicon-based atom chips, with the upper chip referred to as the science-chip and the lower chip referred to as the base-chip, see figure 11a).

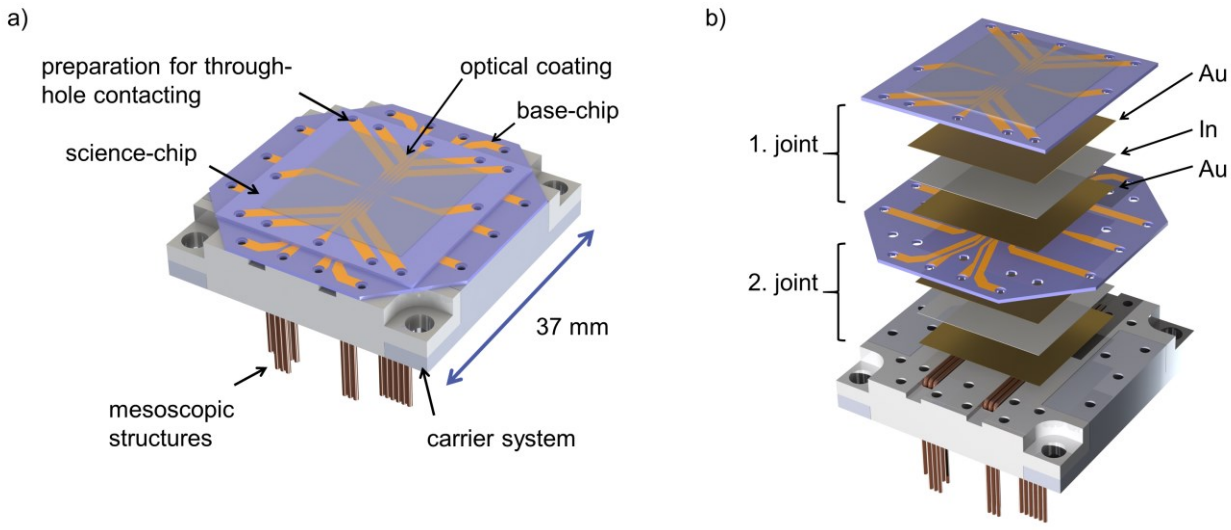

Figure 11. a) Structure of the multilayer atom chip system.
b) Layered structure of the joining layers. [15]

The technologies for manufacturing the atom chips and joining them remain unchanged, and the planar surface of the atom chips easily enables vertical expansion of the system.

Figure 12 shows the first multilayer demonstrator. The optical coating and the pins will be realized in a next step.

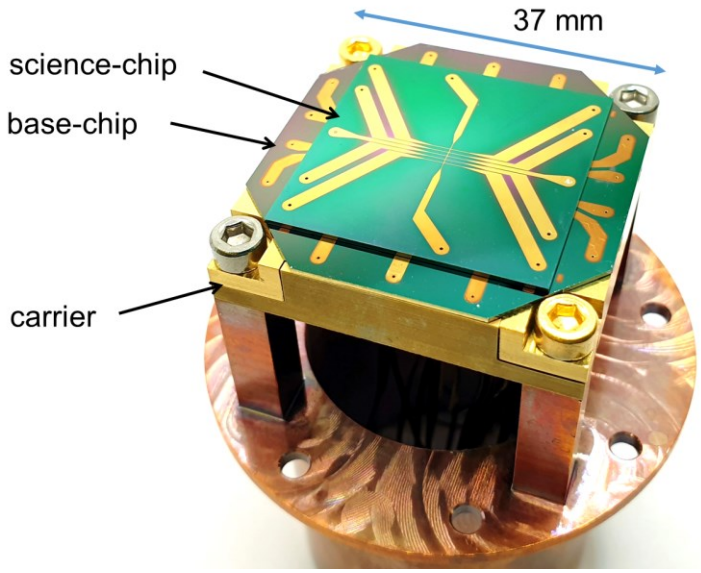

Figure 12. Structure of the multilayer atom chip system.

To qualify the vacuum properties, the atom chips were characterized by the Physikalisch-Technische Bundesanstalt with an outgassing measurement using the accumulation method [16]. A science-chip and two bonded chips (science-chip and base-chip) were evaluated. An atom chip with a transfer coating according to the state of the art [11], [14] served as a reference. Table 1 summarizes the results in terms of outgassing rate and residual gas composition.

Table 1: Outgassing measurement of the atom chips.

	Outgassing rate in mbar·l/s	**Residual gas analysis, composition in %**					
		H_2	**CO_2**	**H_20**	**CO**	**CH_4**	**other**
Science-Chip	4,26E-13	81	7	6	4	1	1
Science+Base-Chip (bonded)	3,14E-13	90	5	1	3	1	0
Atom chip with transfer coating	6,9E-11	20	57	1	19	1	2

4. Periphery for miniaturized quantum systems

In addition to the atom chip as the core component in a miniaturized quantum system, the necessary peripherals require miniaturisation, for example the vacuum technology and the atom source. Packaging and joining processes are being developed for the construction of the MQS that meet the vacuum requirements. As with the atom chips, this includes the use of low-outgassing, non-adhesive joining techniques and the use of vacuum-compatible materials. Since single-stage pumping down to the UHV range is not possible, the MQS is already joined under UHV conditions. Miniaturized pumps will be used to maintain the pressure in the MQS. This means that there is no need for comparatively large, heavy and energy-intensive mechanical backing and high-vacuum pumps. In terms of pressure measurement, the challenge is that vacuum gauges have comparable or even larger internal volumes than the remaining part of the vacuum system, motivating the development of an appropriate pressure measurement device. We present a magnet-free approach based on field emitters, which does not affect the magnetic cleanliness required for operation of the atom interferometer. In addition to the measurement function, this principle allows active pumping at the same time and is similar to the established ion getter pump. A further pumping effect is realized by the use of non-evaporable getters (NEG). For this purpose, we develop so-called NEG microsystems. These NEG microsystems are thermally activated to achieve a constant pumping effect. The local and temporary activation temperature is below 200°C and thus in a range that is not critical for the quantum system. For the realization of the MQS we strive for a modular approach. Modular here means that both the manufacturing technologies (e.g. joining processes) and the system components (e.g. package, getter) can be used together for the application in the MQS. An example is a microheater that is to be used for NEG activation and is thus part of the pump system, but is also used in a miniaturized atom source.

4.1. On the way to the micro quantum system: Metal 3D printed vacuum chambers

In perspective, the goal is to realize a quantum system on a microscopic scale. On the way to this goal, however, the individual components must first be evaluated. For this reason, an intermediate step is to further miniaturize classical CF-based vacuum chambers by using metal 3D printing. We use the laser powder bed fusion (LPBF) process for more freedom in chamber design, optimization of surface structures for weight reduction and rapid prototyping. An example of a weight-optimized component is shown in figure 13.

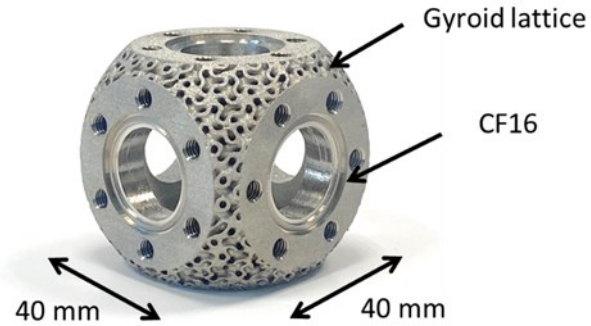

Figure 13. Manufactured vacuum chamber with the LPBF-Process.

3D metal printing is used, for example, to produce the holder for the atom chip system shown in the system in figure 3. In addition, geometries can be created that are not possible using classic CNC machining, such as integrated cooling channels.

4.2. Packaging of quantum sensors on a chip scale

For the fabrication of miniaturized UHV packages, we have developed a UHV bonding stand, the CAD model of which is shown in figure 14. This enables chip-scale packaging of quantum sensors, with encapsulation taking place under UHV conditions. The UHV bonding stand consists of two vacuum chambers, one of which serves as a load lock and the other contains the joining apparatus. Both chambers are each pumped down by a combination of a diaphragm pump and a turbomolecular pump, and the joining chamber is also equipped with an ion getter pump. Both chambers are separated from each other by a UHV slide valve.

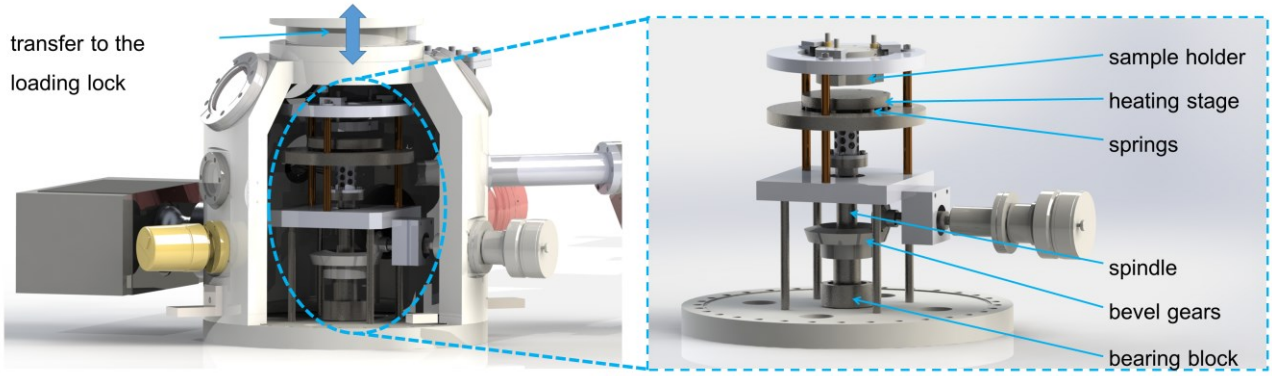

Figure 14. UHV bonding stand for joining the MQS.

The components to be joined in a UHV microchamber are inserted into the loading lock in a separated state and brought into the joining chamber by a UHV manipulator. The holding device for the joining process is shown in figure 15. In the simplest case, the MQS consists

of a base and a lid enclosing a cavity and equipped with the actual quantum system. The individual components must be aligned with each other prior to the joining process. The UHV bonding stand therefore has the capability to manipulate the position of the components to be joined under UHV conditions and to generate appropriate heating and current for the joining process.

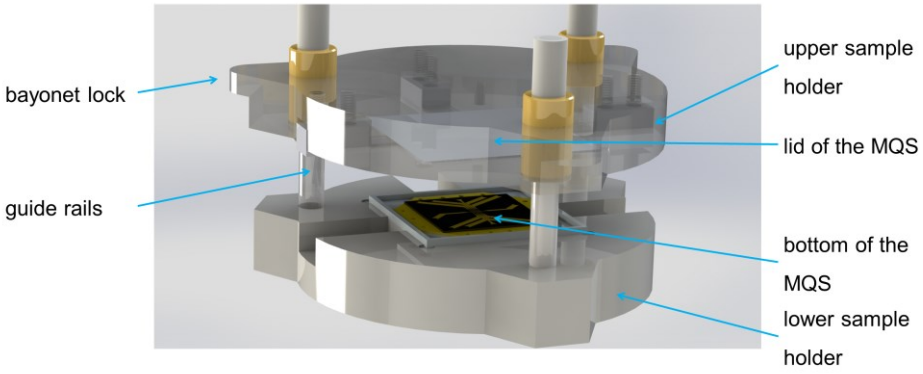

Figure 15. Holding device for joining process.

The guarantee of the boundary conditions necessary for the process will be ensured by continuous monitoring of the process chamber. For this reason, a mass spectrometer is connected to the UHV bonding stand. The presented UHV bonding stand was successfully put into operation and the first results published [17].

4.3. Miniaturized vacuum pumps and measuring systems

After encapsulation in the UHV bonding stand, there is a need to maintain the vacuum in the MQS by means of suitable vacuum technology due to real (permeation) and artificial leakage (outgassing). At the center of this vacuum technology are the novel, miniaturized, non-evaporable getter pumps (NEG microsystems). The principle of operation is the physical and chemical absorption of the residual gases by the elements of the NEG and then storing them deeper within their volume by diffusion based on thermal activation. Materials considered for NEGs include metals and group IV/V alloys such as titanium, zirconium, vanadium and hafnium. For thermal activation, our NEG microsystem has an integrated microheater that enables a defined temperature entry into the NEG layer.

First prototypes qualitatively confirm the functionality of the NEG microsystem in high and ultra-high vacuum. In this regard, the NEG microsystem is fully scalable in size. For the evaluation of the layers, the NEG microsystem was built on a four-inch wafer, shown in figure 16a). Below the NEG layered composite is the microheater, shown in figure 16b). The image of a 3d profilometer can be seen.

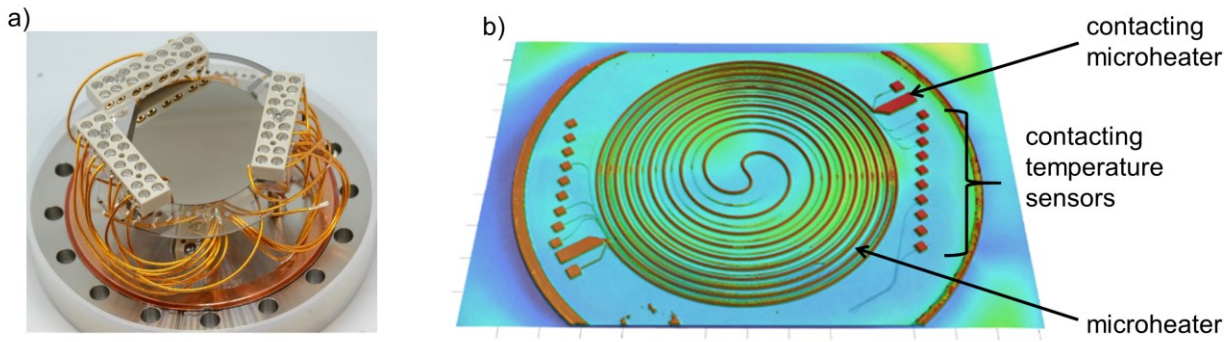

Figure 16. a) High vacuum fixture with built-in getter microsystem.
b) Microheater for activation of the NEG. [18]

Here, the NEG and microheater are electrically insulated from each other. The NEG microsystem can be implemented on an arbitrarily large area, such as on the inside of the lid of the MQS shown in figure 4. NEGs are not a complete solution for a MQS because they are not able to pump alkali vapors or noble gases efficiently. Noble gases and some hydrocarbons, such as methane, are not pumped by NEGs at room temperature. Therefore, sealing under UHV also serves to ensure that most gases are evacuated prior to encapsulation.

To support NEG microsystems and for potential pressure measurement within the MQS, we are working on the development of miniaturized ion getter pumps and ionization measurement devices. Field emitter array electron sources with nanoscale emitter tips, which are micro-engineered, are the basis. The principle of operation is shown in figure 17. An electron source emits electrons that accelerate through a grid to which a positive electrical voltage is applied with respect to the emitter. Ionization of residual gas atoms by collisions subsequently occurs in the vacuum chamber. The ions are then accelerated to the ion collector, which is connected as a cathode, and enter the cathode material. Furthermore, the ion collector can be functionalized with a NEG microsystem to enhance the pumping effect.

The use of field emission instead of thermal emission allows lower temperatures in the quantum system. This is relevant since blackbody radiation affects atoms in free fall [19]. Similarly, our approach avoids the use of permanent magnets, which can affect operation. Figure 18 shows an array of silicon-based field emitter tips and a magnified image of a single tip. The realization is done by reactive ion etching (RIE) after prior masking. We have demonstrated the functional principle of our systems in UHV using exposed emitter tips with external extraction electrodes.

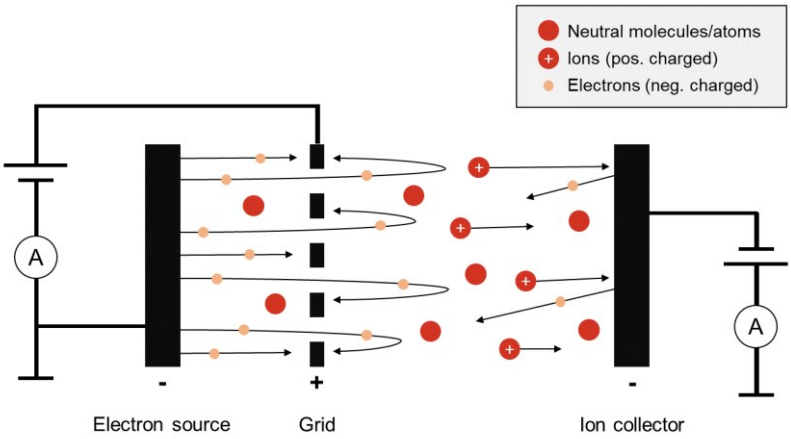

Figure 17. Schematic structure of a miniaturized ion getter pump.

By RIE process optimization we achieve tip radii in the range of less than 50 nm. The process is wafer-level and fully area scalable.

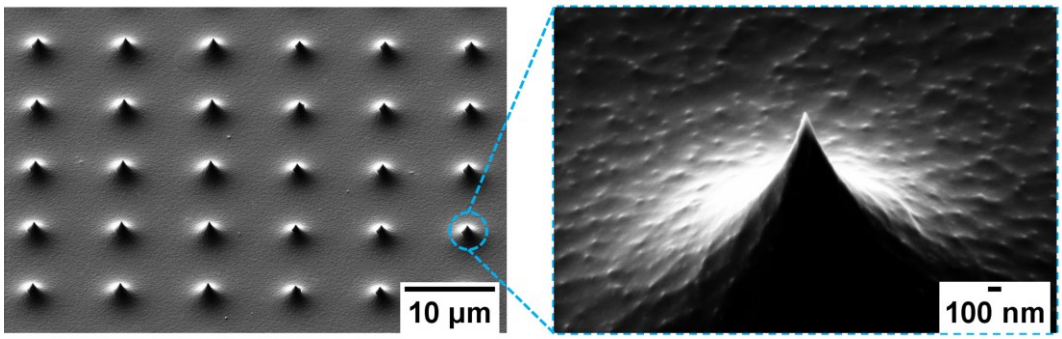

Fig 17. Manufactured field emitter tips.

Our next step at this point is to develop an integrated extraction electrode. The intention is that as the distance between the tip and the extraction electrode decreases, the extraction voltage decreases, so that the pump can be operated with a comparatively low electrical voltage in contrast to the high voltages of conventional ion getter pumps. In addition to the pump effect, the system can also act as a kind of measuring tube. The ionization current allows conclusions to be drawn about the pressure in the vacuum chamber.

5. Conclusion

The presented atom chip system and parts of the periphery will be used in a compact inertial measurement unit based on the multi-axis concept. The atom chip system relies on a polymer-free structure and non-adhesive joining techniques to meet the requirements of the application under UHV conditions. Consequently, the outgassing measurements show an outgassing rate two orders of magnitude lower than atom chips coated with a transfer coating according to the state of the art. Furthermore, the residual gas analysis shows an almost ideal behavior, predominantly H_2 is detected. Both the NEG microsystem and the

miniaturized ion getter pumps are known for their scalability and can be joined into a future miniaturized quantum system by means of the UHV bonding stand, which was also presented.

6. Acknowledgement

This work was supported by the German Aerospace Center (DLR) with funds provides by the Federal Ministry for Economic Affairs and Climate Action (BMWK) due to an enactment of the German Bundestag under Grant No. DLR 50NA2106 (QGyroPlus). Furthermore, we would like to thank Simone Callegari and the Physikalisch-Technische Bundesanstalt for carrying out the outgassing measurements.

References

[1] S. Abend et al. “Atom-Chip Fountain Gravimeter”, *Physical review letters*, *117*(20), pp. 203003, doi: 10.1103/PhysRevLett.117.203003

[2] N. Heine et al. "A transportable quantum gravimeter employing delta-kick collimated Bose–Einstein condensates", *The European Physical Journal D* 74 (2020): pp. 1-8, doi: 10.1140/epjd/e2020-10120-x

[3] C. Freier et al. "Mobile quantum gravity sensor with unprecedented stability", *Journal of physics: conference series*. Vol. 723. No. 1. IOP Publishing, 2016, doi: 10.1088/1742-6596/723/1/012050

[4] R. Karcher et al. "Improving the accuracy of atom interferometers with ultracold sources", *New Journal of Physics* vol. 20, no. 11 (2018): p. 113041, doi: 10.1088/1367-2630/aaf07d

[5] P. Gillot et al. "Stability comparison of two absolute gravimeters: optical versus atomic interferometers", *Metrologia* vol. 51, no. 5 (2014): L15, doi: 10.1088/0026-1394/51/5/L15

[6] C. J. Bordeé, “Atomic interferometry with internal state labelling”, *Phys. Lett. A*, vol. 140, no. 1–2, pp. 10–12, 1989, doi: 10.1016/0375-9601(89)90537-9

[7] M. Kasevich and S. Chu, “Atomic Interferometry Using Stimulated Raman Transitions”, *Phys. Rev. Lett.*, vol. 67, no. 2, pp. 181–184, 1991, doi: 10.1103/PhysRevLett.67.181

[8] M. Gersemann: ‘Atom interferometry with ultracold atoms for inertial sensing’. PhD thesis. Leibniz Universität Hannover, will be published

[9] Gersemann, M., Gebbe, M., Abend, S. et al. “Differential interferometry using a Bose-Einstein condensate“, *Eur. Phys. J. D* **74**, 203 (2020). https://doi.org/10.1140/epjd/e2020-10417-8

[10] A. Kassner et al., “Atom chip technology for use under UHV conditions”, *Smart Systems Integration; 13th International Conference and Exhibition on Integration Issues of Miniaturized Systems, Barcelona, Spain, 2019*, pp. 69–75, ISBN 978-3-8007-4919–5, 2019

[11] R. Folman, P. Treutlein, and J. Schmiedmayer, “Atom Chip Fabrication”, in *Atom Chips*, J. Reichel and V. Vuletić, Eds. Weinheim, Germany: Wiley-VCH Verlag GmbH & Co. KGaA, 2011, pp. 61–117

[12] M. Trinker et al., “Multilayer atom chips for versatile atom micromanipulation”, *Appl. Phys. Lett.*, vol. 92, no. 25, 2008, doi: 10.1063/1.2945893

[13] J. Reichel, W. Hänsel, and T. W. Hänsch, “Atomic micromanipulation with magnetic surface traps”, *Phys. Rev. Lett.*, vol. 83, no. 17, pp. 3398–3401, 1999, doi: 10.1103/PhysRevLett.83.3398

[14] J. Reichel, W. Hänsel, P. Hommelhoff, and T. W. Hänsch, “Applications of integrated magnetic microtraps”, *Appl. Phys. B Lasers Opt.*, vol. 72, no. 1, pp. 81–89, 2001, doi: 10.1007/s003400000460

[15] A. Kassner et al., “Atomchips mit integrierten optischen Gittern zur Erzeugung von Bose-Einstein-Kondensaten Atomchips with integrated optical gratings for the production of Bose-Einstein condensates”, in *MikroSystemTechnik Kongress 2019 - 28. – 30. Oktober 2019 in Berlin*, 2019, pp. 541–544

[16] Callegari, S., “Fundamentals for vacuum experiments for quantum technologies”, 2023; Hannover

[17] N. Droese et al., “Aufbau eines Ultrahochvakuumbonders für das Verkapseln von Quantensystemen” will be published in *MikroSystemTechnik Kongress 2023 - 23. – 25. October 2023 in Dresden*, 2023

[18] L. Diekmann et al. "Nonevaporable getter-MEMS for generating UHV conditions in small volumina", *Journal of Vacuum Science & Technology B,* vol. 40, no. 5, 2022, doi: 10.1116/6.0001991

[19] P. Haslinger et al., “Attractive force on atoms due to blackbody radiation”, *Nat. Phys.*, vol. 14, no. 3, pp. 257–260, 2018, doi: 10.1038/s41567-017-0004-9